MODELING STRONG MOTION DATA FROM THE 1979 IMPERIAL VALLEY EARTHQUAKE

Ralph J. Archuleta(I)
Presenting Author: Ralph J. Archuleta

ABSTRACT

By comparing synthetic particle velocities with the near-source strong-motion data we have constructed, by trial and error, a faulting model for the 1979 Imperial Valley earthquake. The calculation of the synthetic seismograms takes into account the vertical inhomogeneity of the elastic parameters in the Imperial Valley and the spatial variation of the slip-rate parameters on the fault plane. The independent slip-rate parameters are (i) the strike-slip rate amplitude, (ii) the dip-slip rate amplitude, (iii) the duration that slip rate is non-zero (the rise time of the slip function) and (iv) the rupture time, which determines when the slip rate is initiated. Our faulting model has the following principal features: (1) Faulting occurred on the Imperial fault and on the Brawley fault, rupture on the Brawley fault being triggered by rupture on the Imperial fault. (2) The Imperial fault is a plane 35 km long and 13 km wide with a strike of 323°, measured clockwise from north, and a dip of 80° NE. The Brawley fault is a 10 km long and 8 km wide plane with a strike of 360° and a dip of 90°. (3) Faulting on the Imperial fault is primarily right-lateral strike slip with a small component of normal dip slip in the sediments at its northern end. The larger strike-slip rates are generally confined between depths of 5 and 13 km with maximum values of about 1.0 m/s. The duration varies on the fault with a maximum of 1.9 s, which is considerably shorter than the total time for the rupture to take place. (4) The rupture velocity on the Imperial fault is highly variable. Locally it exceeds the shear wave velocity, and in one instance, the compressional wave velocity. The average rupture velocity, though, is less than the shear wave velocity. (5) Although the slip on the Brawley fault contributes only about 4 percent of the total moment, it greatly affects the ground motion at nearby stations. (6) The total seismic moment is 6.7×10^{18} Nm where the Imperial fault contributes 6.4×10^{18} Nm and the Brawley fault contributes 2.7×10^{17} Nm.

INTRODUCTION

In terms of near-source observations of ground accelerations and surface offsets the Imperial Valley earthquake of October 15, 1979, is the best documented earthquake ever recorded (Johnson, et al., 1982). The abundance and quality of these near-source observations presents an unparalleled opportunity for studying the mechanism of a moderate sized earthquake M_L 6.6 (Chavez et al., 1982), $M_o = 7.0 \times 10^{18}$ Nm (Kanamori and Regan, 1982). The results presented in this paper are determined from analysis of an important subset of all the data: time histories of the ground velocities determined from accelerograms recorded in the United States (Brady et al., 1982).

(I) U. S. Geological Survey, 345 Middlefield Road, Menlo Park, CA 94025.

Figure 1 shows a map view of the Imperial Valley with the accelerograph locations relative to the epicenter (Archuleta, 1982a) and to the Imperial and Brawley faults on which surface slip was measurable (Sharp, et al., 1982). Nine additional accelerographs in Baja California,

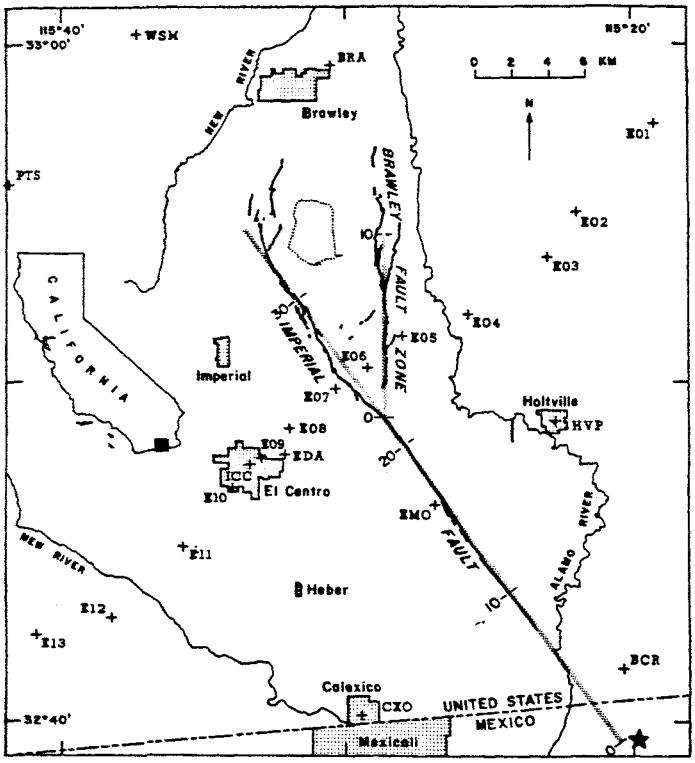

Figure 1. Map view of the Imperial Valley area showing locations of accelerographs in the United States (+'s), parts of the Imperial fault and Brawley fault zone where surface offsets were measured, the location of the epicenter, indicated by a star, and geographical features such as the international border and local communities.The linear stipled regions show the fault traces as we have modeled them. Distances are shown along the traces. The shaded box on the inserted outline of the state of California shows the approximate region for the Imperial Valley area.

Mexico recorded the mainshock (Brune et al., 1982). In this paper we do not consider the Mexican stations though they would probably increase the resolution of the faulting model in the hypocentral area.

The fundamental theorem for kinematic modeling and the basis of our approach is the representation theorem (Maruyama, 1963; Burridge and Knopoff, 1964)

$$\dot{u}_i(\mathbf{y}, t) = \int_0^t dt' \int_A \dot{\mathbf{s}}(\mathbf{x},t',T,\tau) \cdot \mathbf{T}^i(\mathbf{x}, t-t'; \mathbf{y})\, dA \qquad (1)$$

where $\dot{u}_i$ ($\mathbf{y}$, t) is the i'th (i = 1, 2, 3) component of particle velocity at spatial coordinate $\mathbf{y}$ and time t; $\dot{\mathbf{s}}$ ($\mathbf{x}$, t', T, τ) is the slip rate vector at fault coordinate $\mathbf{x}$ and time t'; $\mathbf{T}^i$ ($\mathbf{x}$, t-t'; $\mathbf{y}$) is the traction per unit impulse at the fault coordinate $\mathbf{x}$, due to a point force applied in the i'th direction at the observer location $\mathbf{y}$; dA is an incremental area of the fault plane with total area A; the double integrals are for summation of the kernel over the entire fault plane and the single integral on dt' is for the temporal convolution of $\dot{\mathbf{s}} \cdot \mathbf{T}^i$. The observer coordinates $\mathbf{y}_1$, $\mathbf{y}_2$, and $\mathbf{y}_3$ and the fault coordinates $\mathbf{x}_1$, $\mathbf{x}_2$ share the same origin. We take the point on the Imperial fault's surface trace closest to the epicenter for the origin (Figure 1).

FAULTING MODEL

In the more than 300 faulting models we have tried, almost every parameter has been varied. The Green's functions are computed in the frequency band 0.0-1.0 Hz using the discrete wavenumber/finite element method (Olson et al., 1984). The Green's functions take into account the vertical inhomogeneity of the velocity structure (Archuleta, 1984). We assumed a maximum fault length of 35 km from the epicenter for the Imperial fault. We determined a plane dipping 80° NE with a maximum plunge of 13 km gave the best results. With the elastic properties of the medium and the geometry of the Imperial fault fairly well set, we would assume a slip-rate function $\dot{\mathbf{s}}$ ($\mathbf{x}$, t, T, τ) and compute synthetic seismograms (Spudich, 1981) to be compared with the data. At first we used only the data of E03, E05, E06, E07, E08, E11, HVP and BCR to constrain our selection of $\dot{\mathbf{s}}$ ($\mathbf{x}$, t,T, τ). Later EMO was added and much later in our modeling E04. Thus, the synthetics at E01, E02, EDA, E10, E12, and E13 are predicted from the faulting model determined by the other stations.

Imperial Fault

The spatial distributions of the four slip rate parameters--strike-slip rate amplitude $\dot{s}_1(\mathbf{x})$, dip-slip rate amplitude $\dot{s}_2(\mathbf{x})$, a rupture time T($\mathbf{x}$) from which a rupture velocity is derived, and duration $\tau(\mathbf{x})$-- are shown in Figure 2.

Strike-Slip Rate. The most obvious feature of the strike-slip rate amplitude is the concentration of the largest amplitudes at depths greater than 5 kilometers. We have tailored the strike-slip rate amplitude combined with the duration, discussed below, to approximate the slip distribution observed at the earth's surface (Sharp et al., 1982). Because of the low shear modulus and the slow velocity of rupture in the sediments, the near surface slip rate contributes very little to the radiation. Our modeling efforts imply that the surface measurements provided little constraint on the strike-slip rate parameters. The slip rate is generally quite small for depths less than 5 km. This feature is substantially different from the other faulting models for this earthquake.

Dip-Slip Rate. The distribution of the dip-slip rate amplitudes complements the strike-slip rate. The distribution coincides with observed surface measurements. The maximum dip-slip rate of 0.55 m/s occurs about 30 km from the epicenter and rapidly decreases to zero at about 6 km depth. Because the dip-slip rate is confined to the sediments where the shear modulus is small and the rupture front arrives later, the

radiation due to the dip-slip component of slip rate is small and arrives mostly after the direct S-waves.

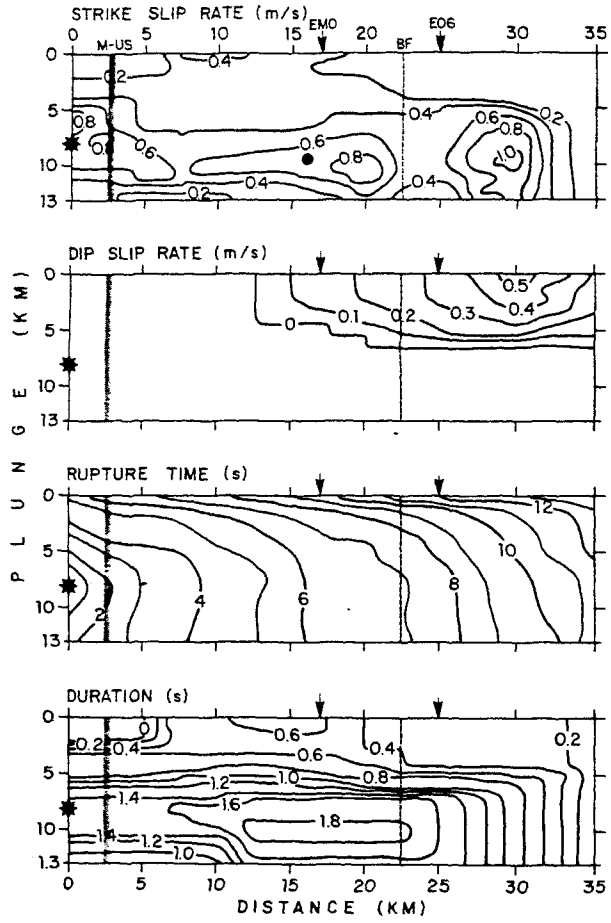

Figure 2. Contours of the slip-rate parameters on the Imperial fault plane. Distances are measured along strike starting at the epicenter and down dip. The hypocenter is shown by the star. The Imperial fault plane dips 80° NE. For reference, the locations of the Mexico-United States border (M-US), Meloland (EMO), E06 and the intersection of the Brawley fault (BF) are shown. The solid circle indicates the hypocenter of the 23:19:35 aftershock.

Duration. The duration grossly resembles the distribution of the strike-slip rate amplitude though the duration is smoother. The duration shows a broad region where it is greater than or equal to 1.5 s with a maximum duration of 1.9 s in the 12-22 km range.

Rupture time. The most unexpected feature of the faulting model is the spatial distribution of the rupture time. The contour lines of rupture time show the position of the rupture front at equal one second intervals of time. Large areas between two successive time intervals indicate a fast rupture velocity and small regions indicate a slow rupture velocity. Unfortunately, the contours do not reveal the complete picture.

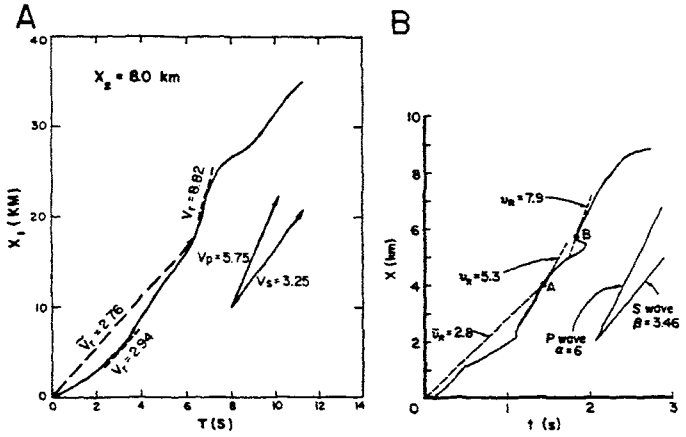

Figure 3. (a) At the hypocentral depth of 8 km, the rupture time is plotted against distance along strike for our faulting model. The secant (average) rupture velocity v_r is simply the position X_1 divided by T (X_1) and is almost everywhere less than the local shear wave velocity. However, the tangent (local) rupture velocity is highly variable, sometimes exceeding the local P-wave velocity. The rupture starts slowly, accelerates, stays nearly constant to about 17 km, suddenly accelerates, then decelerates, then accelerates to a nearly constant velocity. (b) A similar plot is taken from Day (1982) for the case of a spontaneous rupture in the presence of non-uniform prestress. Regions where the prestress are close to the yield stress are the regions with locally supershear and supercompressional rupture velocities. (Reprinted with permission of the Bulletin of the Seismological Society of America.)

Special care must be taken in determining average local rupture velocities near the region, 17.5 - 22.5 km, where the rupture abruptly accelerates. The basic character of the rupture velocity is observed at the hypocentral depth of 8 km (Figure 3). The overall average rupture velocity is 3.1 km/s, which is 0.94 times the local shear wave velocity. In places where the local rupture velocity exceeds the P-wave speed, the rupture process is causal since the average rupture velocity, distance from hypocenter divided by time after origin, is still less than the P-wave speed. Areas of locally fast rupture are simply regions where the stress was relaxed nearly simultaneously. There is an important correlation between the rupture velocity and slip rate amplitude in this model. With the exception of the region near the hypocenter, where the rupture velocity is fast, the slip rate amplitude is high in areas where the rupture is slow, the slip rate amplitude decreases. This correlation is strongest in the 10-30 km

range for depths greater than 5 km. A similar correlation is found in Day's (1982) results.

Static Slip. The static slip is simply the product of slip rate amplitude and duration. Overall, the static slip distribution is similar to the slip rate distribution. The maximum strike-slip offset 1.78 m occurs at 20 km and a depth of 10 km. The maximum dip-slip offset of 0.22 m occurs at the surface. The Imperial fault seismic moment is 6.4×10^{18} Nm.

Brawley Fault. Besides the highly variable rupture velocity on the Imperial fault, the next most unusual aspect was faulting on the Brawley fault zone, (Figure 1). The surface measurements of Sharp et al. (1982) and creep measurements by Cohn et al. (1982) suggested that slip occurred at or near the time that the Imperial fault ruptured. Although slip on the Brawley fault contributed only 4 percent of the total moment, it greatly affects the ground motion at nearby stations (Archuleta, 1984).

SYNTHETIC SEISMOGRAMS

Synthetic particle velocity time histories computed from the combined faulting models for the Imperial and Brawley faults are compared with 48 components of data in Archuleta (1984). The time scale for the data and synthetics is seconds after origin time; the data traces have been aligned according to the trigger time when absolute time was available. For those stations not having absolute time, we shifted the data traces for the best alignment with the synthetics.

Figure 4 shows the data and synthetics at E05, E06, E07, and E08. Except for the 323° component at E08, the synthetics fit the data reasonably well. There are four features to note. First is the 323° component at E06 and E07. Although by theory this component should be practically nodal for a rupture on the Imperial fault, it clearly is not, nor is it antisymmetric even though from the location of E06 and E07 it should be nearly so. This occurs because this component is influenced by rupture on the Brawley fault. The second element is the vertical fit. Although it is far from perfect, the synthetics and data at E05, E07, and E08 show a definite similarity. In particular, the first energy arriving at about 9 seconds is associated with the large amplitude vertical accelerations. The source of this energy is the fault area on which the local rupture velocity is extremely fast and variable. The third aspect is that on the 53° component, the synthetics show the same amplitude and double-sided character as the data. The strike-slip rate concentrations have amplitudes about 0.8 m/s. Since geometrical spreading attenuates the amplitude by 1/R, the fact that the lowpassed particle velocities have maximum amplitudes about 0.8 m/s suggests that there is a considerable amount of constructive interference of waves from different parts of the fault. The last feature to note is the small pulse in the data, arriving at about 18-20 seconds on the 53° component. This pulse, observable in the synthetics, is SS. The amplitude of this pulse is strongly dependent on the slip-rate amplitude in the sediments. To match the synthetic SS pulse with the data requires the model to have small slip-rate amplitudes at depths shallower than 5 km.

SUMMARY

Using a trial-and-error forward kinematic modeling, we computed synthetic particle velocity time histories to compare with the observed lowpassed near-source velocities of the 1979 October 15 Imperial Valley earthquake. Radiation from rupture on the Imperial fault dominates almost all the near-source ground motion. However, about eight seconds after its origin time, rupture on the Imperial fault triggered rupture on the Brawley fault. Radiation from the Brawley fault severely affects certain components of motion at several nearby stations. The total combined moment of the Imperial and Brawley faults is 6.7 x 10^{18} Nm, which is very close

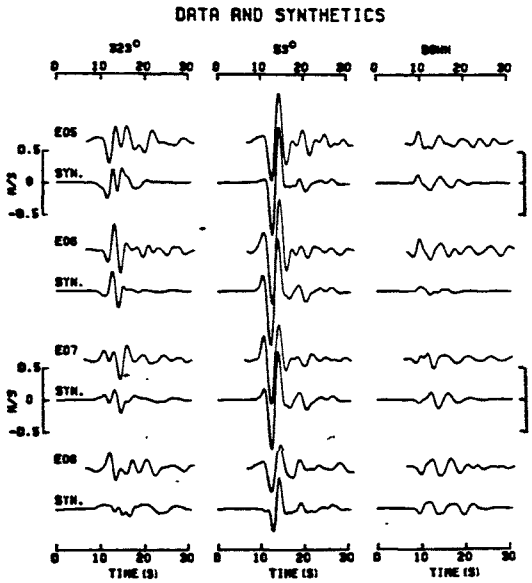

Figure 4. Comparison of three components of synthetic particle velocity time histories with the data at Stations E05, E06, E07 and E08. All components are plotted to the same amplitude scale.

---

to the seismic moment of 7 x 10^{18} Nm determined by Kanamori and Regan (1982) from long period surface waves. Perhaps the most unsuspected feature of the 1979 Imperial Valley earthquake is the complex temporal evolution of the faulting is described through the rupture time parameter. Of the four faulting parameters we most often varied, the synthetics were most sensitive to changes in the rupture time parameter. An expanded version of the analysis in this paper is found in Archuleta (1984).

REFERENCES

1. Archuleta, R. J., Hypocenter for the 1979 Imperial Valley earthquake, Geophys. Res. Letters, 9, 625-628, 1982a.
2. Archuleta, R. J., Analysis of near-source static and dynamic measurements from the 1979 Imperial Valley earthquake, Bull. Seism. Soc. Am., 72, 1927-1956, 1982b.

3. Archuleta, R. J., A faulting model for the 1979 Imperial Valley Earthquake, in press, Journal of Geophysical Research, 1984.
4. Brady, A. G., V. Perez, and P. N. Mork, Digitization of processing of mainshock ground-motion data from the U. S. Geological Survey accelerograph network: The Imperial Valley, California, Earthquake, October 15, 1979, U. S. Geological Survey Professional Paper 1254, 377-384, 1982.
5. Brune, J. N., F. L. Vernon, III, R. S. Simons, J. Prince, and E. Mena, Strong-motion data recorded in Mexico during the main shock: The Imperial Valley, California, Earthquake, October 15, 1979, U. S. Geological Survey Professional Paper 1254, 319-350, 1982.
6. Burridge, R., and L. Knopoff, Body force equivalents for seismic dislocations, Bull. Seism. Soc. Am., 54, 1875-1888, 1964.
7. Chavez, D., J. Gonzales, A. Reyes, M. Medina, C. Duarte, J. N. Brune, F. L. Verson, III, R. Simons, L. K. Hutton, P. T. German, C. E. Johnson, Mainshock location and magnitude determination using combined U. S. and Mexican data: The Imperial Valley, California, Earthquake, October 15, 1979, U. S. Geological Survey Professional Paper 1254, 51-54, 1982.
8. Cohn, S. N., C. R. Allen, R. Gilman, and N. R. Goulty, Pre-earthquake and post-earthquake creep on the Imperial fault and the Brawley fault zone: The Imperial Valley, California, Earthquake, October 15, 1979, U. S. Geological Survey Professional Paper 1254, 161-168, 1982.
9. Day, S. M., Three-dimensional simulation of spontaneous rupture: the effect of nonuniform prestress, Bull. Seism. Soc. Am., 72, p. 1881-1902, 1982.
10. Johnson, C. E., C. Rojahn, and R. V. Sharp, editors, The Imperial Valley, California, Earthquake, October 15, 1979, U. S. Geological Survey Professional Paper 1254, 1-451, 1982.
11. Kanamori, H., and J. Regan, Long-period surface waves: The Imperial Valley, California, Earthquake, October 15, 1979, U. S. Geological Survey Professional Paper 1254, 55-58, 1982.
12. Maruyama, T., On the force equivalents of dynamic elastic dislocations with reference to the earthquake mechanism, Bulletin Earthquake Research Institute, Tokyo University, 41, 467-486, 1963.
13. Olson, A. H., J. A. Orcutt, and G. A. Frazier, The discrete wavenumber finite element method of synthetic seismograms, Geophys. J. R. Astr. Soc., in press, 1983.
14. Sharp, R. V., J. J. Lienkaemper, M. G. Bonilla, D. B. Burke, B. F. Fox, D. G. Herd, D. M. Miller, D. M. Morton, D. J. Ponti, M. J. Rymer, J. C. Tinsley, J. C. Yount, J. E. Kahle, E. W. Hart, K. E. Sieh, Surface faulting in the central Imperial Valley: The Imperial Valley, California, Earthquake, October 15, 1979, U. S. Geological Survey Professional Paper 1254, 119-144, 1982.
15. Spudich, P. K. P., The deHoop-Knopoff representation theorem as a linear inverse problem, Geophys. Res. Letters, 7, 717-720, 1980.
16. Spudich, P., Frequency domain calculation of extended source seismograms, EOS, 62, 960, 1981.